Development of a method for measuring organic compounds in ice samples using PTR-ToF-MS

Leon Saris
Meteorology, Physical Oceanography and Climate

August 2014

Dr. Rupert Holzinger
Institute for Marine and Atmospheric research Utrecht (IMAU)

Abstract

The uncertainty of the past aerosol composition affects the reliability of estimates made of their effect on Earth's radiation budget. In this report, a method to measure organic compounds in ice samples by using a Proton-Transfer-Reaction Time-of-Flight Mass-Spectrometer (PTR-ToF-MS) will be presented. A "PTR-ice" device has been developed to separate soluble and insoluble organics and to remove bulk water from the samples prior to the analysis with PTR-ToF-MS. The "PTR-ice" system has been validated and compared with offline TD-PTR-MS measurements [Timkovsky et al., 2014] of ambient filter samples from the CESAR-observatory near Cabauw, Netherlands. Improvements in bulk water removal was obtained by using evaporation through a dry air flow instead of extracting moisture by creating a vacuum. Artefacts resulting from the rather large inner surface of the "PTR-ice" are demonstrated and useful insights have been gained on how to reduce these. A definite measurement method has yet to be found, however improvements on the measurement of organic compounds in ice samples are shown.

Universiteit Utrecht

Contents

1 Introduction

The definition of aerosols, according to the IPCC 4th Assessment Report, is:

> *A collection of airborne solid or liquid particles, with a typical size between* 0.01 µm *and* 10 µm *that reside in the atmosphere for at least several hours. Aerosols may be of either natural or anthropogenic origin. Aerosols may influence climate in several ways: directly through scattering and absorbing radiation, and indirectly by acting as cloud condensation nuclei or modifying the optical properties and lifetime of clouds.*

As can be read in the definition, aerosols are an interesting, but complex part of the climate system. Both in present day climate, as in the past climate, the effect of aerosols on the radiation balance has its uncertainties. This is mainly due to an unclear pre-industrial aerosol load and composition and an uncertain aerosol-cloud interaction.
Aerosol species that are entrained by atmospheric moisture may be deposited on a glacier. With an increasing duration, the precipitation on the glacier accumulates forming an archive of past precipitation and its aerosol species. Not only by precipitation, the aerosol species or its gaseous precursors may be deposited on the glacier. By interaction with the ice, by dry deposition or by filtration of particles blown through the firn layer, the concentration of aerosol species may increase. With a lower rate of precipitation, a higher concentration is expected since there is more dry deposition per unit volume. With a reconstruction of the amount of precipitation, for the mass load of the organics in the atmosphere can be deduced[Legrand and Mayewski, 1997].
The goal of the methods introduced in this report is to allow not only the measurement of the insoluble organic compounds in ice samples, it allows the measurement of water soluble organics as well. The mass load as well as the distinction between multiple water soluble and water insoluble organics can than be made and quantified.
In the first section of this report the formation and deposition of aerosols will be presented, a summary on the climate effects and how much is known of aerosols so far. After this three different measurement methods will be presented (section 4.1 to section 4.3) which were contrived to obtain a measurement method for the composition of organics in ice from which past organic aerosol composition can be reconstructed. I will wrap up in section 5 with the conclusions of my research on how to measure the past organics content from ice records.

2 Aerosols

2.1 What are aerosols?

Aerosols can be formed either through direct emission to the atmosphere or they can be formed chemically in the atmosphere itself. The indirect formation is a gas-liquid or gas-solid transition. Aerosols emitted directly are referred to as primary aerosols (PA) and aerosols formed indirectly in the atmosphere are referred to as secondary aerosols.
Aerosols can not only be discriminated by their formation, another division is by their chemical contents: either organic or inorganic. Organic aerosols are particles consisting mainly out of carbon, hydrogen and oxygen. Other particles are the inorganic particles, like Sahara dust and many forms of salts, like common sea salt (NaCl), ammoniumsulfate ($(NH_4)_2SO_4$) and ammoniumnitrate (NH_4NO_3).
The main focus of this research will lie on the secondary organic aerosols (SOA). The formation of SOA (both formed in the atmosphere and consisting mostly out of carbon, hydrogen and oxygen) is by oxidation of volatile organic compounds (VOC)[Gelencsér, 2004]. VOC's can be from various biogenic and anthropogenic sources. These precursor gasses become oxidised by reacting with hydroxyl radicals (OH)[Grosjean and Seinfeld, 1989; Izumi and Fukuyama, 1990]. The now oxidised volatile organic compounds are decreased in volatility allowing them to condense on other particles forming a SOA (either on PA or SOA), as is shown schematically in figure 1.

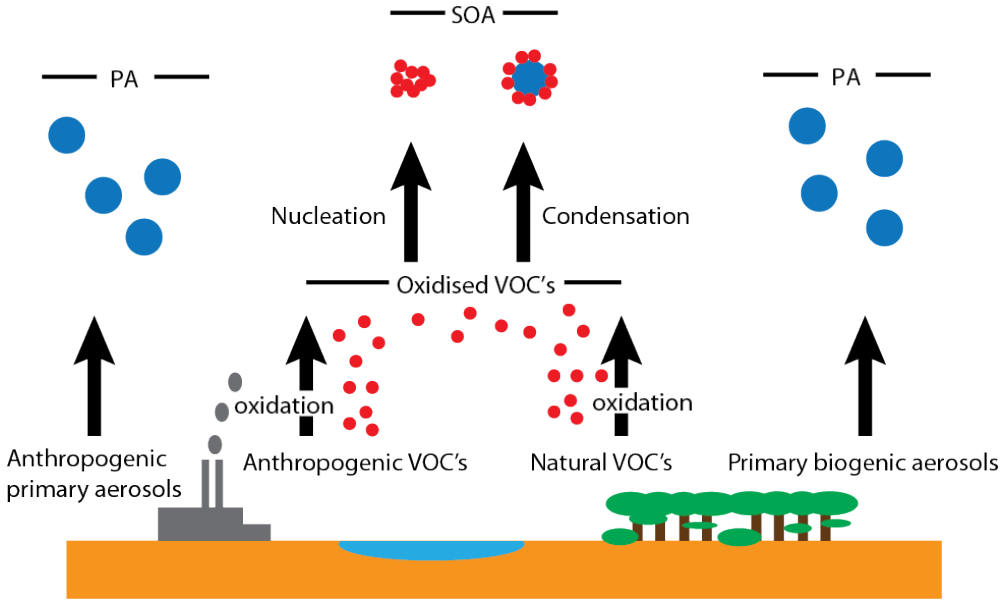

Figure 1: The emission of primary aerosols and the formation mechanism of SOA. The emission of VOC's lead, through the oxidation of these compounds to SVOC where SOA is formed through either nucleation of condensation.

Carbonaceous particles can be subdivided in two groups. The organic carbon (OC) and black carbon (BC) or elemental carbon (EC). The distinction between OC and BC or EC is operationally defined. BC is defined by it's relatively high absorption of radiation and EC is defined by it's relatively high refractiveness of radiation, all other carbon is defined as OC. There is, however, a slow transition between OC and BC or EC[Pöschl, 2005]. The total carbon is the sum of OC and BC or the sum of OC and EC.
The removal of the particles can occur via either chemical decomposition or by dry/wet deposition. Chemical decomposition is where aerosol particles react to become gaseous species. The deposition term which can either be through dry deposition, where the particles simply fall on the Earth's surface due to gravity and surface roughness effects, or by wet deposition. In a supersaturated environment, aerosols may act as cloud condensation nuclei (CCN) or ice nuclei (IN). This means atmospheric moisture may condensate on the particle. As more moisture condensates, a droplet or ice crystal is formed. With increasing moisture, the

total mass of both the particle and the moisture is increased. Either the water evaporates again from the particle, or the particle will precipitate down on the surface. This is known as wet deposition. Since the process of deposition is different, as well as the characteristics on which the deposition depend, chemical decomposition, dry deposition and wet deposition is usually considered separately. The average lifetime of aerosol particles, from formation or emission to deposition or decomposition, is typically 3 to 10 days.

2.2 The effect of aerosols

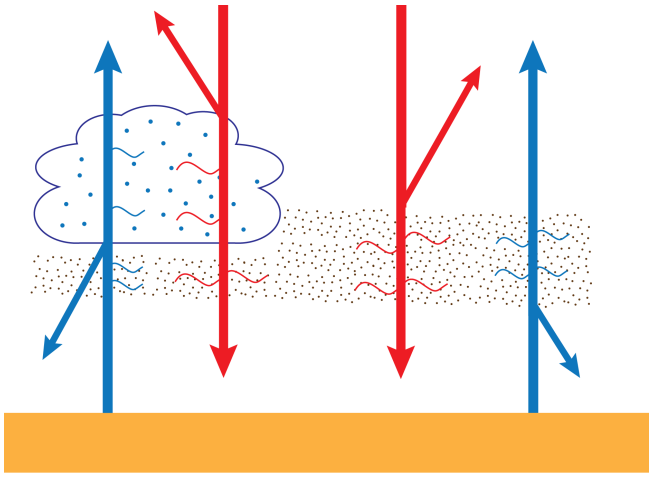

Figure 2: The influence of aerosols on the radiation budget of the Earth. Red arrows indicate incoming (shortwave) solar radiation and blue arrows indicate outgoing (longwave) radiation. Due to absorbance of aerosols energy dissipates in the aerosol-containing layer.

Aerosols interact in multiple ways with both shortwave and long wave radiation. and therefore affect the radiation balance on Earth. In figure 2 the effects of aerosols is schematically shown. The arrows represent either incoming or outgoing radiation. Aerosols interact with the surroundings by absorbing and reflecting incoming (solar) radiation and outgoing (longwave) radiation, as can be seen on the r.h.s. of the figure. This is referred to as the primary aerosol effect. Furthermore, aerosols interact with atmospheric moisture by acting as CCN or IN. This leads to the formation of cloud(droplet)s. Cloud droplets reflect and absorb radiation more effectively than the dry aerosol particles, since the increased size of the particles. In addition to this, clouds formed with an increased number of aerosols tend to have smaller droplets that precipitate less easily and therefore increase the lifetime of the aerosols. These effects are referred to as the secondary aerosol effect.

Different aerosols affect the radiation budget differently. Particles may absorb more radiation than other particles, which reflect more or interact with atmospheric moisture differently. The total effect of the radiative influence of aerosols is shown in figure 3. As we can see, the aerosols have an estimated overall cooling effect on the Earth's climate. The uncertainties in both the primary effect and the secondary effect is very high. The uncertainty could mean that the cooling effect due to aerosols could be twice as large as well as aerosols leading to a mean global radiation increase. The level of confidence reflects the level on which expert opinions agree to the estimated forcing. Which is high for the primary effect and low for the secondary aerosol effect. The regional effect of aerosols on the climate, however, is not shown here. The prolonged lifetime of clouds does not only affect the radiation balance, land use may be changed as well since the location where there is precipitation may shift due to this increased lifetime.

Not only do aerosols affect the climate, an increased concentration of fine air particulate matter are correlated with severe health effects, including enhanced mortality rate, cardiovascular, respiratory and allergic diseases (e.g. [Brunekreef and Forsberg, 2005]).

Aerosols may as well affect tourism by decreasing visibility. The scattering of solar radiation by aerosols limits visibility in the troposphere. In particular, when the relative humidity is high, the optical thickness increases due to water uptake, decreasing visibility. For example in figure 4, the Grand Canyon national park can be seen and how an increased haze may decrease the line of sight dramatically[Doyle and Dorling, 2002; van Beelen and van Delden, 2012].

Since aerosols act as CCN, the particles may be encapsulated in water droplets. These droplets may precipitate on the surface, containing the CCN as well as particles caught during flight. Past precipitation may be stored on mountain glaciers which can be used as an archive of past aerosol particles. When the particles can be subtracted from the ice, a mass spectrometer could measure the components of the particles contained.

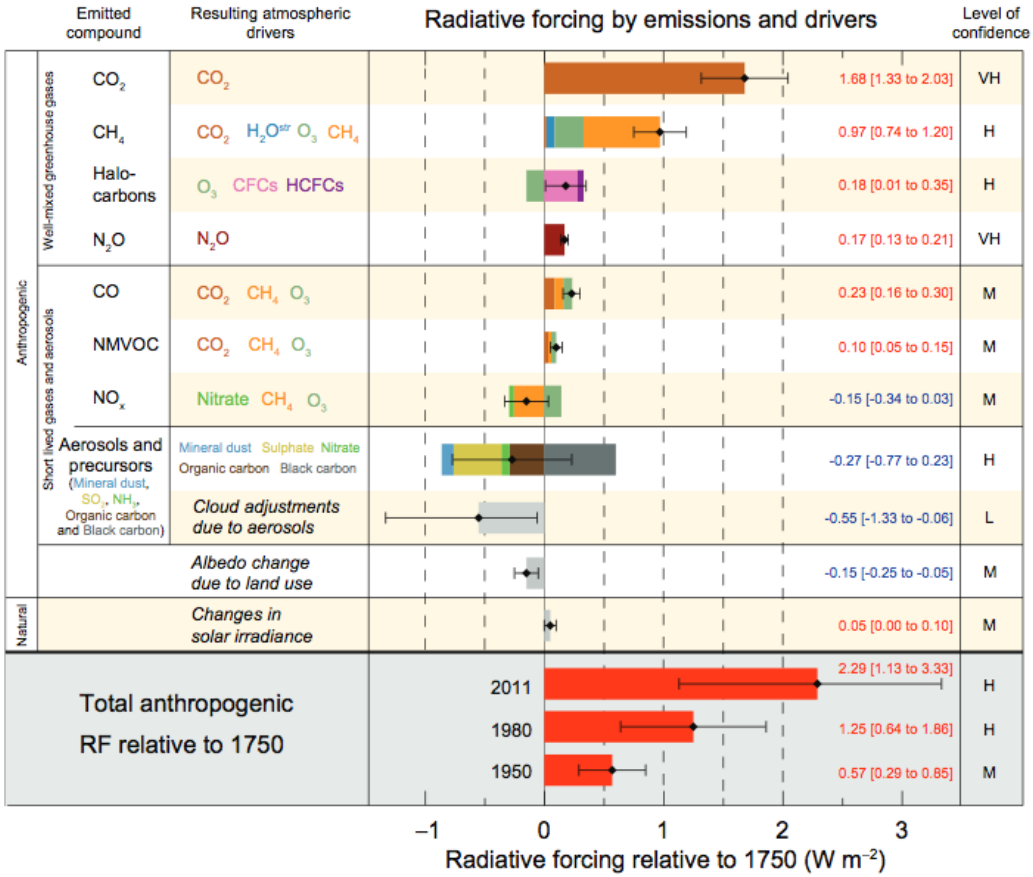

Figure 3: The globally averaged radiative forcing[IPCC, 2013]. Bars indicate the individual contributions to the radiative forcing of different components to the climate system relative to the radiative balance in 1750. The error bars show the accuracy with which the forcing is estimated. The black diamonds is corresponds to the estimated forcing with the corresponding level of confidence which is shown in the last column. (VH–very high, H–high, M–medium, L–low, VL–very low). For three different years (1950, 1980 and 2011) the total anthropogenic forcing relative to 1750 is provided.

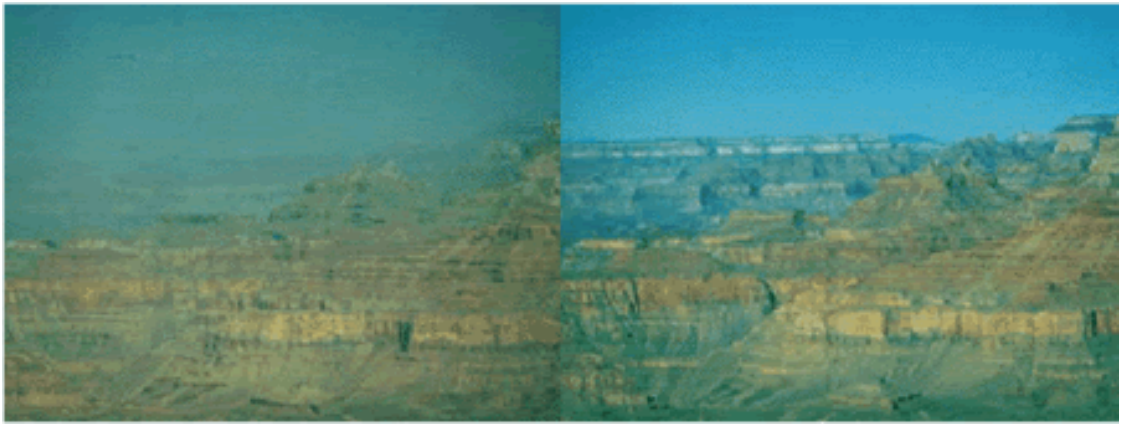

Figure 4: Difference between a decreased sight and a clear sight in the Grand Canyon. Photo by US EPA AIRTrends 1995 Summary

2.3 Past composition

Only since the coming of satellite imagery a global scale record of aerosol load in the atmosphere is present. In the pre-sattelite era there are no estimates of the total amounts or the composition of aerosols, although an indication can often be given by the measured aerosol optical thickness (AOT). Most recently, filtration of ice samples provide measurements of the insoluble components of the aerosols. Beside this, few measurements exist and most knowledge of the past composition is based on model studies. In these models, the present day pristine conditions with an anthropogenic impact are scaled to the Earth's population[Dentener et al., 2006]. Aerosols have a relatively short lifetime. Measurements done therefore are only a regional image of the aerosol components. The local knowledge of the changing aerosol content provide the necessary data for input or validation of models[Boucher et al., 2013].

3 Experimental

3.1 PTR-ToF-MS

The main advantage of this mass spectrometer, the Proton Transfer Reaction-Time of Flight-Mass Spectrometer (PTR-ToF-MS), is the ability to discriminate chemicals with a high precision with a real-time measurement. In the PTR-ToF-MS, which is shown schematically in figure 5, the compounds are ionised and measured using a time of flight mass spectrometer. The compound's ionisation is initiated by the ionised water molecules. The ionisation takes place in the ion source. This water is ionised according to either of the following reactions:

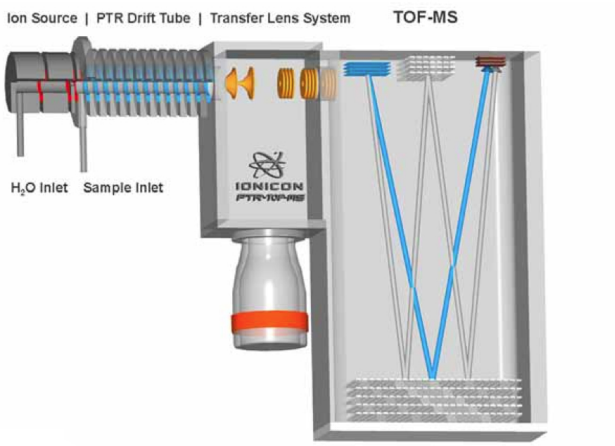

Figure 5: Schematic view of the PTR-TOF-MS [1]

$$\begin{aligned} H_2O + e^- &\longrightarrow H^+ + OH + 2\,e^- \\ H_2O + H^+ &\longrightarrow H_3O^+ \end{aligned}$$

$$\begin{aligned} H_2O + e^- &\longrightarrow H_2O^+ + 2\,e^- \\ H_2O^+ + H_2O &\longrightarrow H_3O^+ + OH \end{aligned}$$

$$\begin{aligned} H_2O + e^- &\longrightarrow H_2^+ + O + 2\,e^- \\ H_2^+ + H_2O &\longrightarrow H_3O^+ + H \end{aligned}$$

$$\begin{aligned} H_2O + e^- &\longrightarrow OH^+ + H + 2\,e^- \\ OH^+ + H_2O &\longrightarrow H_3O^+ + O \end{aligned}$$

A hollow cathode provides high energy electrons interacting with the water molecules present in the ion source chamber. With an electric force, the H_3O^+-ions are forced towards the drift tube and non-H_3O^+-ions are filtered due to an intermediate chamber after which only the H_3O^+-ions remain. In the drift tube the ions interact with the sample (the to be measured compounds). When a sample-molecule (R) has a higher proton affinity (PA) than the H_3O^+-ions, the H_3O^+ interacts with R, forming both H_2O and RH^+:

$$H_3O^+ + R \longrightarrow H_2O + RH^+$$

The sample RH^+ can now, again with an electrical field, be forced to the transfer lens system where the ions are bundled in a focused beam towards the ToF-MS. In this final chamber the ions are forced to follow a known path. Since all ions receive equal energy, a direct relation between the time of flight and the mass to charge ratio, m/z, can thus be found.
Due to reduced mobility, the PTR-ToF-MS has a decreased precision when measuring in moist conditions[Dotan et al., 1976; Viehland and Mason, 1995]. In addition to this, the water molecules in the sampled air interact with the ions as well.[de Gouw and Warneke, 2007]

$$\begin{aligned} H_3O^+ + nH_2O &\longleftrightarrow H_3O^+(H_2O)_n \\ RH^+ + nH_2O &\longleftrightarrow RH^+(H_2O)_n \end{aligned}$$

The main challenge of measuring the aerosols in ice is to filter enough water out the sample to obtain a sufficient mass load for every ion above noise levels. Water in the PTR-ToF-MS may as well cluster around

[1] Source: Ionicon, `http://www.ionicon.com/information/technology/expert-information`

the ions and therefore increase the measured ion's molecular weight. Therefore, for our measurement of the organics in the glacier archives, the water needs to be extracted from the samples to measure accurately. After this has been done, the particles can be evaporated by heating, to measure the gaseous compounds with the PTR-ToF-MS.

3.2 offline TD-PTR-MS

The offline – Thermal Desorption – Proton Transfer Reaction – Mass Spectrometer (offline TD-PTR-MS, from here on referred to as TD-PTR-MS), as described by Timkovsky et al. [2014], enables us to measure captured organics with the PTR-ToF-MS. The sampled air can, therefore, be measured off-site multiple times with high precision. In figure 6 (bottom) the TD-PTR-MS is shown schematically. The samples air filter can be inserted in the filter holder and inserted in a cylindrical quartz glass tube with inner diameter of 8.8 mm. The filter holder is inserted up to Oven 1, with length 10 cm where the temperature increases with steps of 50 °C, from 100 °C to 350 °C. Per time step taking approximately 10 s after which the temperature is maintained for an approximate 170 s before increasing to a next temperature. This can be seen schematically in figure 6 (top). The Oven 2 temperature is kept at a constant 200 °C to prevent condensation of the volatized gasses. As a carrier gas, a 50 mL min^{-1} nitrogen flow is maintained (unless stated otherwise, volume flow rates refer to STP). The PTR-ToF-MS was loosely attached to the TD-PTR-MS sampling only a fraction of the N_2-flow.

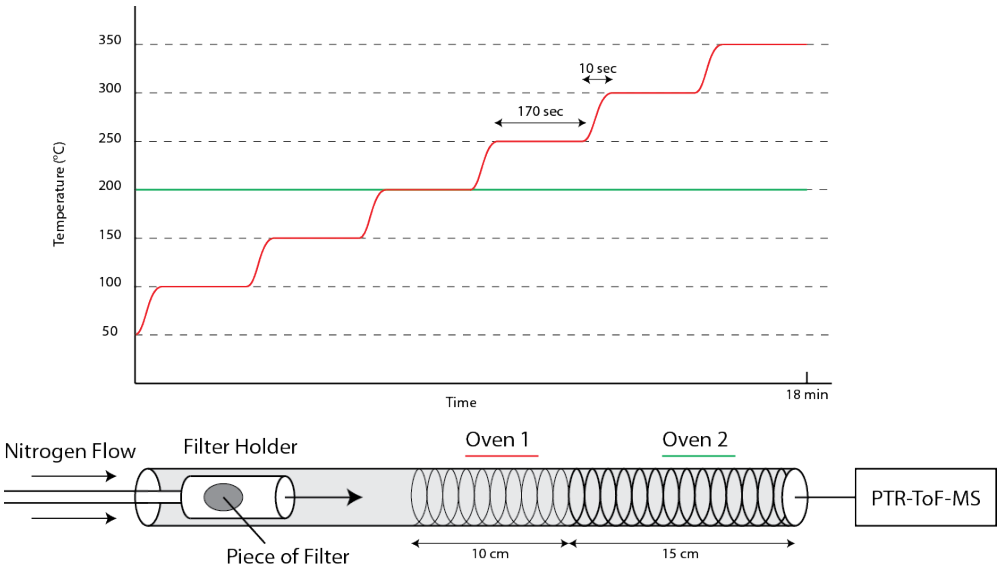

Figure 6: Bot: Schematic view of the offline TD-PTR-MS [Timkovsky et al., 2014]. Top. The temperature of Oven 1 (red) and Oven 2 (green) over time with typical timespans indicated.

3.3 PTR-ice

The PTR-ice is developed to remove excess moisture from a sample before measuring the sample to enable high precise measurements with the PTR-ToF-MS. One clear application for this would be the water content removal from a glacier sample, to measure the past organics content. The PTR-ice is shown schematically in figure 7. The sample with excess moisture can be inserted in the Top chamber. The moisture will sink to the Bottom chamber. Large, insoluble particles will remain in the Top chamber due to the presence of a filter (Bekipor 3AL3, 3 µm pores). In the bottom chamber the moisture is removed by a vacuum pump. The N_2-inlet and the PTR-ToF-MS connections are closed to create a flow from the air inlet to the vacuum pump taking away the high humidity air from the PTR-ice. After a pressure of 31 mbar is reached at the pressure meter, the Air in/outlet is closed to evaporate the remainder in a near-vacuum. At a pressure of 2.1 mbar the excess moisture content is considered to be removed. The residue in the chambers is the to be measured particulate matter. With a constant 110 mL min^{-1} nitrogen overflow originating at the N_2 source and the excess N_2 leaving the system at the Air in/outlet, resulting in a 23 mL min^{-1} semi-constant flow through the PTR-ice system.

For the particles to evaporate, the temperature of both chambers is increased. Starting with both chambers at a 50 °C temperature, the top chamber is heated at a constant 13 °C min^{-1} temperature rate to a 250 °C maximum. Keeping the temperature in the top chamber at a constant 250 °C, the bottom chamber is heated afterwards. From an equal 50 °C initial temperature to a higher 300 °C with an equally set 13 °C min^{-1} temperature increase per minute. A typical temperature profile is given in figure 8. To keep recondensation in the PTR-ice to a minimum a Sulfinert (Restek) coating is applied.

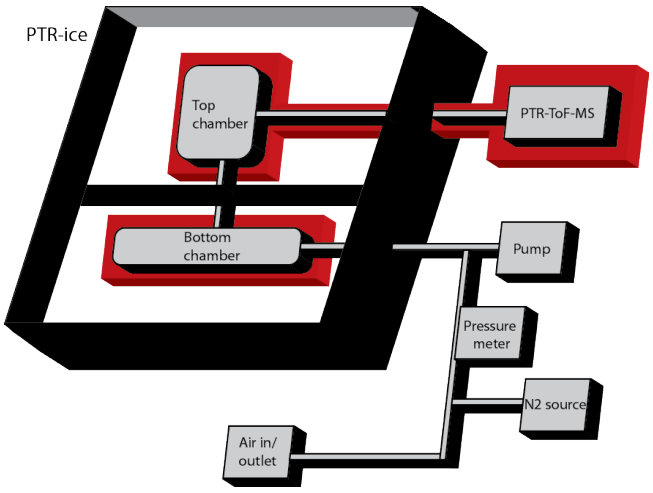

Figure 7: A schematic view of the PTR-ice. Highlighted in red are the areas where the temperature can be set manually. Top chamber, bottom chamber and PTR-ToF-MS can be set to separate temperatures.

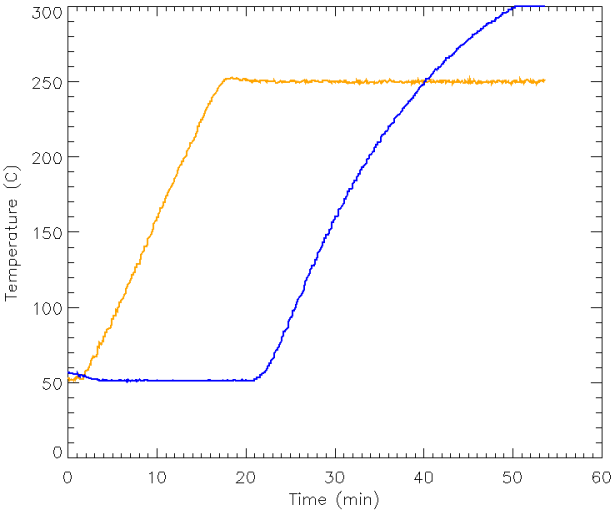

Figure 8: A typical temperature profile. Orange the temperature profile for the top chamber and blue the temperature profile for the bottom chamber.

3.4 Samples used

The measurements done with the PTR-ice were compared with the measurements done with the TD-PTR-MS[Holzinger et al., 2010a,b; Timkovsky et al., 2014]. The efficiency of the PTR-ice is validated by comparing replicate filter samples measured by both.
The effect of a measurement in the PTR-ice with respect to the measurement done by the TD-PTR-MS is compared under three different conditions: (a) dry, (b) the effect of the evaporation of water and (c) the effect of melting ice and evaporate the water. For this cause aliquots of a filter sample were used which are (a) kept dry (b) are blended with milliQ water and (c) are blended with milliQ water and frozen afterwards. The three measurements done with the PTR-ice will then be compared to dry filters measured by the TD-PTR-MS.
Air filter measurements obtained at a rural site near the Cabauw Experimental Site for Atmospheric Research (CESAR)[2] (N 51.58.198 E 4.55.583) were used, which is surrounded by the Randstad, consisting of large cities as Amsterdam, Rotterdam, The Hague and Utrecht at distances around 30 km to 40 km. Furthermore, surrounding the site at approximately 10 km to 30 km are highways. A high volume sampler (Digital HVS model DHA 80) was used to collect aerosols using a 500 L min^{-1} steady airflow. The airflow is forced through circular quartz fiber filters (Whatman, QMA) with a 150 mm diameter, of which 140 mm was exposed to the airflow.
In table 1 the samples used, as well as their sampling date and time, are shown.

Sample code	Starttime	Endtime	Specifics
24	2 May 2011, 15:15	4 May 2011, 14:25	Continuously
89	2 December 2011, 09:15	8 December 2011, 13:30	Continuously
118	17 May 2012, 19:00	20 May 2012, 07:00	Night, Blank
129	1 July 2012, 07:00	3 July 2012, 19:00	Day
130	1 July 2012, 19:00	3 July 2012, 07:00	Night

Table 1: The air filters sample code and their measurement day and time. In specifics is indicated whether there was continuously sampling, during 12 hours at night (19:00 - 07:00), or during 12 hours during the day (07:00 - 19:00).

Samples were kept in pre-treated aluminium foil (heated at 500 °C for a minimum of 3 hours) and conserved at −20 °C in air-tight polyethylene bags. The stamp and tweezers to cut the filters were cleaned with both acetone and ethanol. The filters were circularly cut to a 1 cm diameter. Blanks are treated equally, only no particles are collected during the sampling period.
The filters are inserted in the filter holder as indicated in figure 6. This is compared to the measurement done with the PTR-ice. A "dry" measurement, where the filter is inserted in the PTR-ice directly. A "liquid" measurement, where plastic tubes (Greiner, 188 271) were rinsed with milliQ water, afterwards cleaned ultrasonically in milliQ water for 30 minutes and finally rinsed with milliQ water again. Filters were added, together with either 2 mL or 5 mL of milliQ water to the tubes. A 10 h minimum was maintained for the particulates to solve in the water before measurement. As a third, an "ice" measurement, is an similar treatment to "liquid", however, 20 h after adding the filter to the milliQ water in the tubes the samples were frozen at −20 °C.
The "liquid" and "ice" are, as the "dry" measurement inserted to the top chamber of the PTR-ice and evaporated, as explained in section 3.3.

[2] http://www.cesar-observatory.nl/

3.5 Data treatment

The data is processed for easy handling as described in Holzinger et al. [2010b]. The program Interactive Data Language (IDL, version 8.1,ITT Visual Information Solutions) was used for data analysis. All measurements were analysed together to produce a unified mass list containing volume mixing ratios (*VMR*) of the ions measured. The *VMR*'s for every ion, for every measurement, were averaged to a mean value per 50 °C timestep (*AVMR*). All ions with a lower mass to charge ratio (m/z) than 40 Da are discarded due to saturation of the PTR-ToF-MS by the primary ion signal. Per ion the 5th percentile was subtracted to account for instrumental backgrounds.
The mass concentration per time step (C_i), with i the time step, is then calculated according to equation 1:

$$C_{n,i} = AVMR_{n,i} \times M_i \times F_{inlet,n} \times t_n / S \tag{1}$$

with per measurement, n, and per ion, i, the average volume mixing ratio $AVMR_{n,i}$, the molecular weight for every ion M_i, the Nitrogen inlet flow, $F_{inlet,n}$, the measurement time, $t_{n,i}$, and the measured sample's surface area, S. Unless noted otherwise, measurements were done in threefold and the median value per time step was taken to obtain one value - per time step - per ion - per measurement - for further analysis. Measurements were not adjusted to the corresponding blank measurement. Afterwards the time steps are added to obtain a single mass load per ion's measurement:

$$C_i = \sum_{n=1}^{N} \text{Median}\left(C_{n,i,1}, C_{n,i,2}, C_{n,i,3}\right) \tag{2}$$

With N is the maximum amount of time steps relevant to the measurement (often up to 250 °C for the top chamber and 300 °C for the bottom chamber). This C_i is the mass load per ion.
A ratio is defined where the mass load of an ion of a first method is divided by the mass load of an ion of a second method. For every ion a different ratio can therefore be defined.

4 Results

4.1 PTR-ice

4.1.1 The setup

The samples used are filter number 118, 129 and 130. Sample code numbers 129 and 130 both were mixed in threefold with 5 mL milliQ water and for sample code numbers 129 and 130 there were three samples mixed with 5 mL milliQ water and frozen afterwards. Measurements proceeded as described in appendix A.
The settings for the PTR-ToF-MS used are shown in table 2. 83340 individual spectra were averaged over time to obtain a time resolution of 5 s.

Table 2: Input variables for PTR-ToF-MS.

Pdrift	2.4 mbar
H_2O	4.0 sccm
Us	140 V
Uso	130 V
Udrift	600 V
Udx	35 V
Ihc	6 mA
DTC	120 °C
ITC	180 °C

4.1.2 Measurement

A total of 1108 different ions were discriminated. In figure 9 the ratio of different measurement techniques for all measured ions is shown. On the left hand side (l.h.s.) the measurements of sample code 129 and on the right hand side (r.h.s.) the measurements of sample code 130 is shown with from top to bottom the comparisons between measurement techniques.
For both sample codes 129 as 130, it comes to eye that the comparison in figures 9a and 9b, which is the comparison of TD-PTR-MS and PTR-ice, provides ions with relatively high mass loading for the PTR-ice:dry measurement around a ratio of 0.3. This would mean that, on average, the current PTR-ice:dry technique measures only 30% of the mass loading per ion measured compared to the TD-PTR-MS.
When the figures 9c and 9d are reviewed, the loss in mass load continues. A further fraction of 0.470 and 0.660 is the measured median value for sample code 129 and 130, respectively. On top of that, the spread of the median 50% is increased to 0.854 for sample code 129 and 0.860 for sample code 130.
Regarding figure 9e and 9f, especially at the measurement of sample code 130, the ratio's between the measured mass loadings with the sample frozen compared to the sample solved in water is around 1 (the median for sample code 129: 1.146 and for sample code 130: 0.954). The spread of the median 50% remained, for the sample code 130 measurement at 0.240, which would indicate a small deviation from the PTR-ice:liquid measurement. The liquid samples are therefore likely not largely affected by the freezing and melting process.
To validate this, three subsequent measurements of PTR-ice:dry are regarded and compared them to the median value of the three measurements. When a single measurement is consistent to the median value of the three measurements (which is what is expected) a large number of ions will have a ratio of 1.0 (and thus a strong increasing blue line at ratio 1.0). This intercomparison is shown in figure 10 and, as can be seen in the top figures, there is indeed a spread strongly surrounding the ratio of 1.0 with the median values being respectively 0.772, 1.002 and 1.190. The figure on the l.h.s. has a slightly decreased measured mass loading and the figure on the r.h.s. has a small increase in mass loading resulting in similar ratio translations. The difference between the maximum and minimum ratio for the median 50% of all ions is reviewed (and is shown within the brackets in the caption of figure 10). For the PTR-ice:dry a mean ratio difference of 0.19 ((0.288+0.024+0.258)/3) and for the TD-PTR-MS a mean ratio difference of 0.10 ((0.112+0.056+0.128)/3) is observed. The median 50% of the PTR-ice:dry have a larger spread than the TD-PTR-MS with a factor 2 difference.
In figure 11 (bottom figures) the 421 organic compounds contributing to 90% of the total measured mass loading by PTR-ice:dry is shown (top figures). The spread in the measured ratio's between the different techniques is lower (0.216 and 0.148) than in the unadjusted figure with all the ions present (0.272 and 0.256). However, the median ratio between the two measurement techniques is decreased as well, indicating that the compounds with a high ratio consist of a small mass load. When we now regard the bottom figures (378 organic compounds), the median value decreases by interpreting solely the heavy 90% of the PTR-ice:dry. Interestingly, the spread in the median 50%, is much lower (0.140 and 0.094). These results

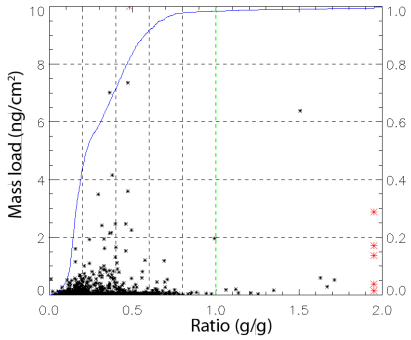

(a) PTR-ice:dry & TD-PTR-MS. Sample 129. [0.226;0.272]

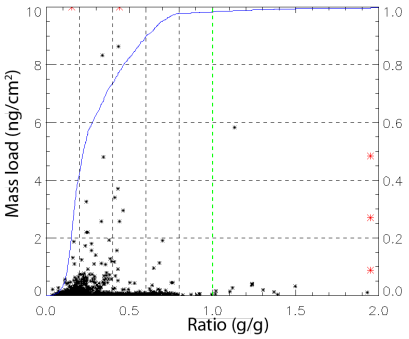

(b) PTR-ice:dry & TD-PTR-MS. Sample 130. [0.226;0.256]

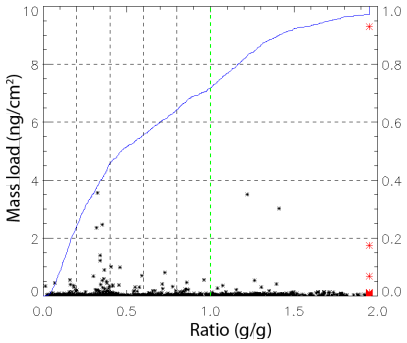

(c) PTR-ice:liquid & PTR-ice:dry. Sample 129. [0.470;0.854]

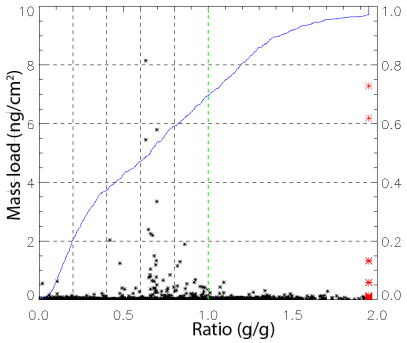

(d) PTR-ice:liquid & PTR-ice:dry. Sample 130. [0.660;0.860]

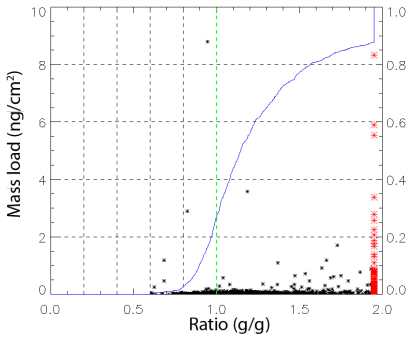

(e) PTR-ice:ice & PTR-ice:liquid. Sample 129. [1.146;0.478]

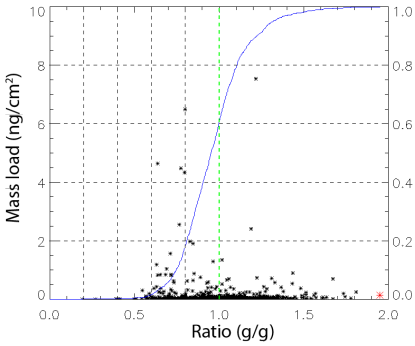

(f) PTR-ice:ice & PTR-ice:liquid. Sample 130. [0.954;0.240]

Figure 9: On the horizontal axis the ratio of the first method divided by the second method (respectively to the sub-caption). The green line indicates the ratio of 1. On the left vertical axis, the total mass loading (on a cm^2 of filter) per ion measured of the method first given in the figure's caption is shown. The black points indicate the corresponding ratio and mass loading per measured ion. The red points are transposed from outside the plot range to the edge of the plot. The blue line indicates the cumulative number of ions measured (from 0 to 1), as is indicated on the right vertical axis. A strong increase indicating a high number of ions measured with the specific ratio.
For sample code number 129 (left) and sample code number 130 (right), figures show from top to bottom the comparison PTR-ice:dry & TD-PTR-MS, PTR-ice:liquid & PTR-ice:dry and PTR-ice:ice & PTR-ice:liquid. The first number inside the caption's square brackets indicates the median value of all organics' ratio and the second number is the maximum difference in ratio for the median 50% of all organics.

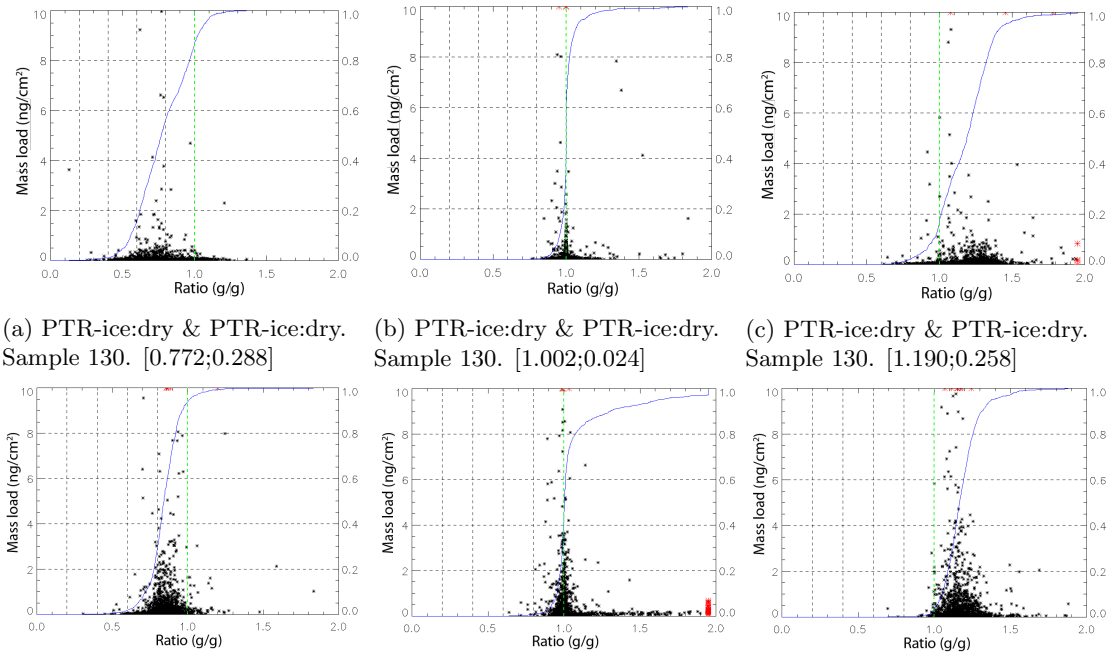

(a) PTR-ice:dry & PTR-ice:dry. Sample 130. [0.772;0.288]

(b) PTR-ice:dry & PTR-ice:dry. Sample 130. [1.002;0.024]

(c) PTR-ice:dry & PTR-ice:dry. Sample 130. [1.190;0.258]

(d) TD-PTR-MS & TD-PTR-MS. Sample 130. [0.842;0.112]

(e) TD-PTR-MS & TD-PTR-MS. Sample 130. [1.004;0.056]

(f) TD-PTR-MS & TD-PTR-MS. Sample 130. [1.166;0.128]

Figure 10: Axis as in figure 9. The comparison of three replica's to the median value of the three individual measurements is shown. On the top row the measurement with the PTR-ice:dry is compared. On the bottom row, the measurements of the TD-PTR-MS is compared to their median value.

imply that the PTR-ice:dry measures more organics with a small mass load.

Since the results of figure 9 suggested that a significant fraction of mass is lost in the PTR-ice, a repetition of measurements deemed necessary. Sample code 130 was measured again, with slightly different settings for the PTR-ToF-MS compared to table 2. The source for the primary ion signal, H_2O, is now increased from 4.0 sccm to 5.0 sccm and the drift pressure (pdrift) is increased to 2.8 mbarSince the PTR-ice:liquid measurement corresponds strongly to the PTR-ice:ice measurement, but both compare poorly with the measurement methods without water included, no measurements were done with filters for a second time that have been dissolved in milliQ water and frozen afterwards. Again the measurement was in threefold and for the PTR-ice:liquid sample, there was 5 mL milliQ water used to mix the dry filter with.
In figure 12 the measurements with the increased primary ion signal is shown. When the comparison between PTR-ice:dry and TD-PTR-MS is regarded, the ratio between the two has increased. From an original median of 0.226 to a new median of 0.444 with no large difference in the spread of the median 50% (from 0.256 to 0.212). On the bottom the m/z-value against the ratio is shown. No apparent trend can be observed. There is an overall loss independent of the m/z value. A loss to recondensation on the internal surface or the inability to evaporate from this surface could be the cause of this loss.
The top-r.h.s. figure shows the comparison between PTR-ice:liquid and PTR-ice:dry. A high number of organics are found to have a ratio of either around 0.2 or a ratio of around 0.5. This is reflected in the bottom figure on the r.h.s. where the mass to charge value is around 0.2 for organics with a m/z-value lower than 400 Da and around 0.5 for organics with a m/z-value above 400 Da. Under the m/z value of 400 Da there are 549 compounds with a ratio lower than 0.2 where there are 14 compounds below this ratio above the m/z value of 400 Da. A significant decrease in ratio for the light compounds which could possibly be appointed to the evaporation with a vacuum pump. This is a rough way of evaporation in which small droplets containing organic material could be dragged along.

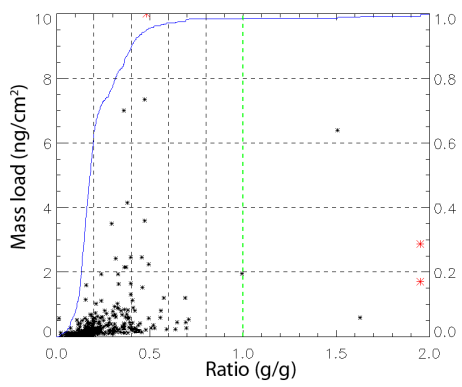

(a) PTR-ice:dry & TD-PTR-MS. Sample 129. Heavy 90% of TD-PTR-MS [0.210; 0.216]

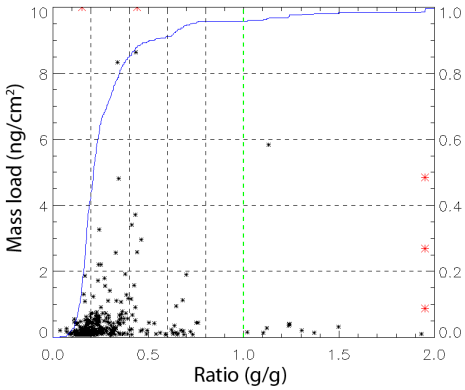

(b) PTR-ice:dry & TD-PTR-MS. Sample 130. Heavy 90% of TD-PTR-MS [0.214; 0.148]

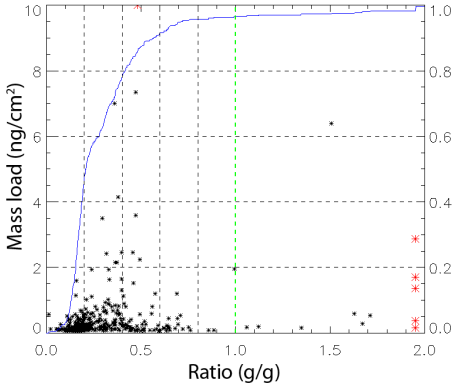

(c) PTR-ice:dry & TD-PTR-MS. Sample 129. Heavy 90% of PTR-ice:dry [0.180; 0.140]

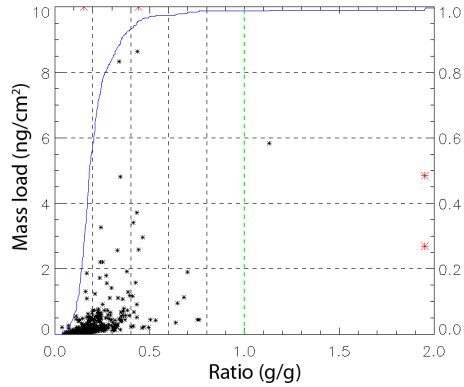

(d) PTR-ice:dry & TD-PTR-MS. Sample 130. Heavy 90% of PTR-ice:dry [0.182; 0.094]

Figure 11: Axis as in figure 9. For the measurements of sample number 129 (left) and sample number 130 (right). The top figures regard the ions composing 90% of the total mass of the TD-PTR-MS measurement. The bottom figures do the same for the PTR-ice:dry measurements.

4.1.3 Conclusion

The measurements done with the TD-PTR-MS have been compared with the newly designed PTR-ice. Since large losses were found a repetition of measurements was done with an increased primary ion signal. With the primary ion signal increased the PTR-ice:dry measurements got closer to the values of the TD-PTR-MS measurements with the ratio of 0.444, but large losses remain (approximately 56%). Possibly the condensation of compounds on the internal surfaces or the inability to evaporate from it may form a loss term which can be seen in the mass load measured.
The measurement of PTR-ice:liquid, where water is included, further decreased the mass load. The method of creating a vacuum in the PTR-ice might be too aggressive. When evaporating the water with a vacuum pump boiling water may spatter and therefore whole water droplets (including organics) may be removed. A possible solution might be to evaporate the water with a softer approach using dry air. Furthermore, a significant loss with ions with a small m/z value, 400 Da, (and therefore often a high solubility) is shown supporting the hypothesis that organics are lost during the rough evaporation of the current PTR-ice:liquid technique.
To further address the encountered problems a soft evaporation technique in section 4.2 has been used and insight has been gain in section 4.3 on how to tackle the internal surface losses by using a more inert surface.

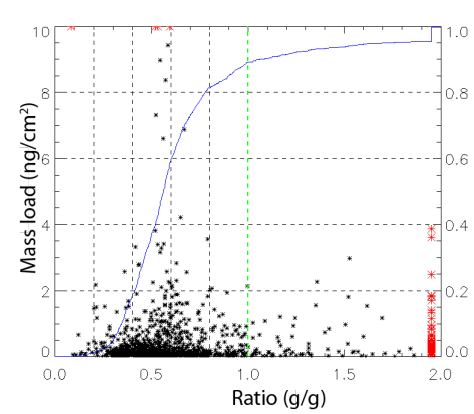

(a) PTR-ice:dry & TD-PTR-MS. Sample 130. [0.444;0.212]

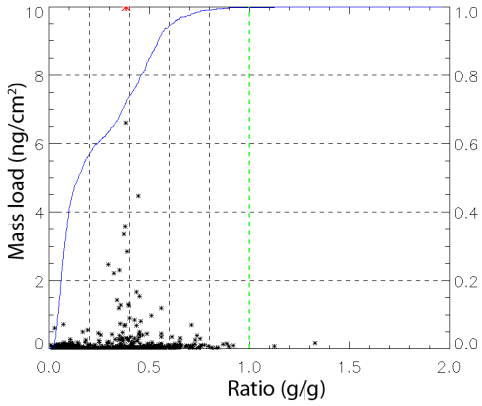

(b) PTR-ice:liquid & PTR-ice:dry. Sample 130. [0.192;0.426]

ion

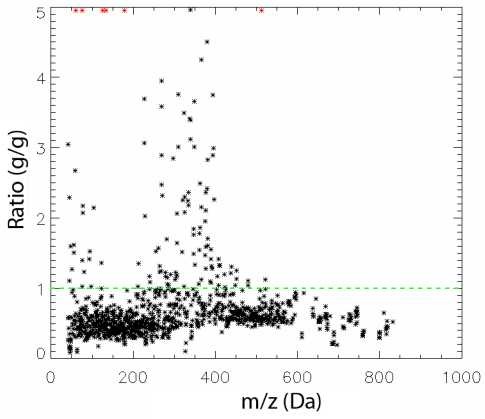

(c) PTR-ice:dry & TD-PTR-MS. Sample 130.

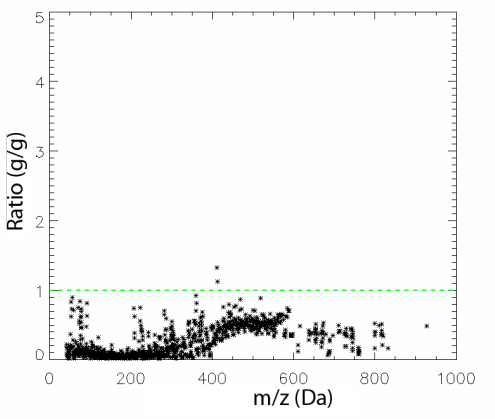

(d) PTR-ice:liquid & PTR-ice:dry. Sample 130.

Figure 12: Top: axis as in figure 9. On the bottom, the m/z value (in Da) with on the vertical axis the ratio between two measurement techniques per ion. The green line indicates a mass load ratio of 1. The figures on the left are a comparison between PTR-ice:dry and TD-PTR-MS and the two figures on the right shown a comparison between PTR-ice:liquid and PTR-ice:dry. Measured with an increased primary ion signal.

4.2 Bulk water removal using dry air flow

4.2.1 The setup

Since evaporation of water using a vacuum pump seemed too rough (as is shown in section 4.1) a softer approach seems necessary. Due to measurement-time considerations slow evaporation by either external sample handling or by evaporation via diffusion is, without consideration of it's efficiency, disregarded. Instead, the use of a dry air flow was introduced to the PTR-ice system (figure 13). Pressurised air, cleaned with both a carbon filter (50 cm charcoal) and a 7 µm particle filter (Swagelok), dry air was blown through the PTR-ice system to evaporate the water in the bottom chamber. The airflow is from the top chamber, through the bottom chamber to exit at the Air in/outlet. The relative humidity (RH) at the Air in/outlet is measured. When a RH of less than 6% is reached, the water is assumed to be evaporated. After evaporation of the water, the measurement continues as described in appendix B.

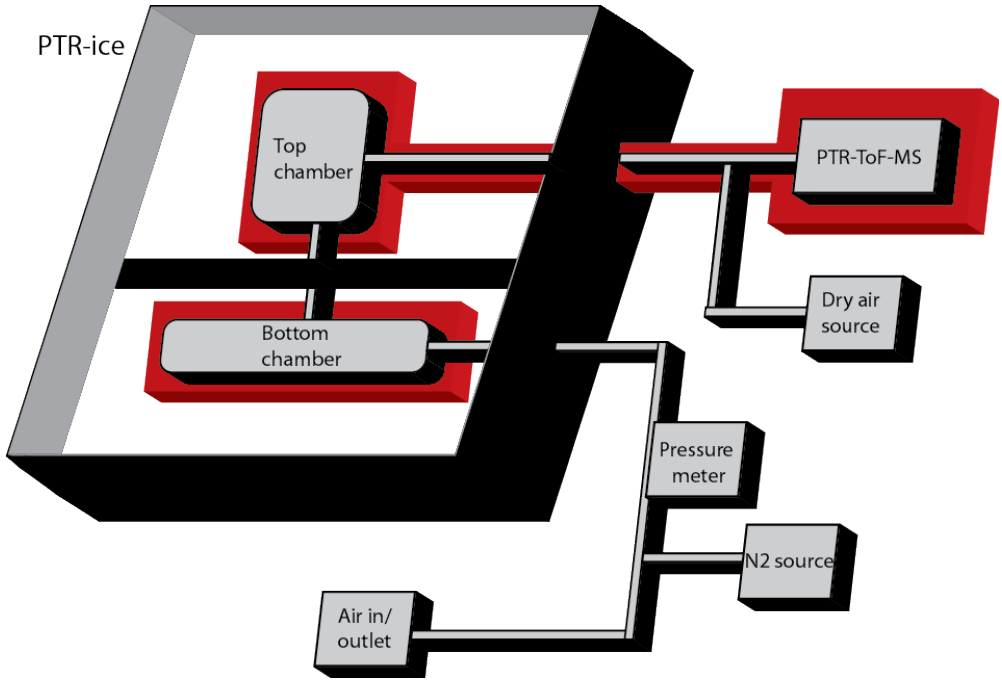

Figure 13: A schematic view of the PTR-ice. Highlighted in red are the areas where the temperature can be set manually. Top chamber, bottom chamber and PTR-ToF-MS can be set to separate temperatures.

Filters with sample code 24 were used for this new measurement procedure. 12 cut filters were mixed with 5 mL milliQ water. Besides that, 3 filters were used for a measurement with TD-PTR-MS and 3 filters were used for PTR-ice:dry measurements. Multiple flow velocities of the dry air and multiple temperatures in the PTR-ice system to evaporate the water were used.

Table 3: Input variables for PTR-ToF-MS.

Pdrift	2.8 mbar
H_2O	5.0 sccm
Us	140 V
Uso	130 V
Udrift	600 V
Udx	35 V
Ihc	6 mA
DTC	120 °C
ITC	180 °C

4.2.2 Measurement

In table 3 the set parameters for the PTR-ToF-MS is shown. Again, a N_2 flow of 110 mL min^{-1} resulting in a similar overflow was used. The temperature increase is again, as in section 4.1, for both chambers with a temperature increase of 13 °C min^{-1}. The different temperatures for evaporation are 30 °C, 40 °C, 50 °C and with flow rates 5.0 L min^{-1}, 10.0 L min^{-1}, 15.0 L min^{-1}, 20.0 L min^{-1}. Each combination of these parameters was measured

once, meaning that 12 different measurements can be compared to the dry measurements. This comparison is shown in figure 14. A total of 1563 different organics were identified.
The results shown are to be compared to the old method of evaporation, with a vacuum pump, which can be seen in figure 12d. Where the median ratio of the vacuum-method was measured to be approximately 0.3, the median has shifted for the dry air-method towards a ratio between 1.1 and 1.6 for all temperatures and flow rates. At a m/z-range of 300 Da, there is for all measurements a ratio increase measured, which has it's possible cause in contamination by the dry air flow. Although no apparent relation between the evaporation duration and contamination at a m/z-range of 300 Da could be found.
Under different temperatures and flow rates the use of dry air to evaporate bulk water is a significant improvement over the vacuum pump method. For a flow rate of $10\,\mathrm{L\,min^{-1}}$ 350 different organics have a ratio between 0.8 and 1.2 compared to the PTR-ice:dry measurement. A relation between the temperature and the median ratio was found, but a temperature of 30 °C is preferred. A low evaporation temperature decreases the evaporation of organics, since the volatility is dependent on the temperature. A higher mass load is expected to remain in the device to be measured later.

4.2.3 Conclusion

Multiple measurements were conducted showing a significant improvement in evaporating the bulk water with dry air over the usage of a vacuum pump resulting in a median ratio increase of 1.1 to 1.6. A flow rate of $10\,\mathrm{L\,min^{-1}}$ is favoured to evaporate the water most effectively. The temperature of evaporation is preferred to keep at 30 °C. Primarily because with an increasing temperature, the vapour pressure of the organics increase and losses are expected to be higher at a high temperature. For this flow rate and temperature, the median obtained is 1.195 with the median 50% organics having a minimum-maximum difference in ratio of 0.935.
An increase in the ratio of the ions with a m/z of approximately 300 Da is possibly due to an increase in contamination due to the dry air source, although no further validation could be found to support this hypothesis.

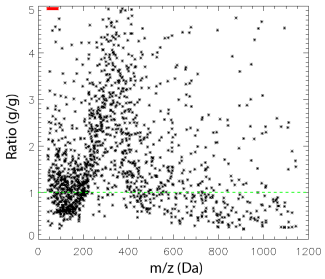

(a) 30 °C, 5 L min^{-1}, 53 min [1.500; 1.690]

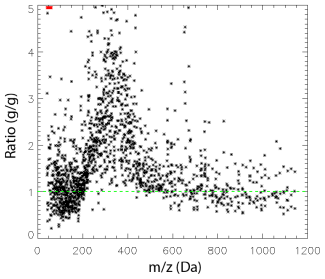

(b) 40 °C, 5 L min^{-1}, 32 min [1.435; 1.155]

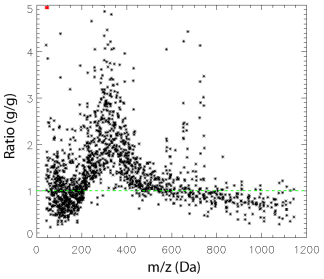

(c) 50 °C, 5 L min^{-1}, 35 min [1.235; 0.890]

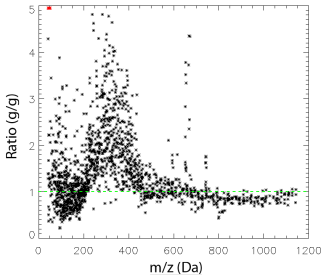

(d) 30 °C, 10 L min^{-1}, 27 min [1.195; 0.935]

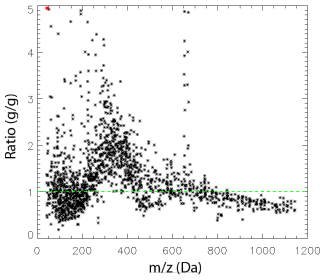

(e) 40 °C, 10 L min^{-1}, 16 min [1.150; 0.815]

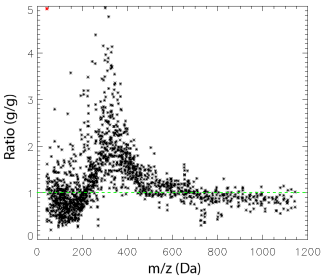

(f) 50 °C, 10 L min^{-1}, 28 min [1.100; 0.715]

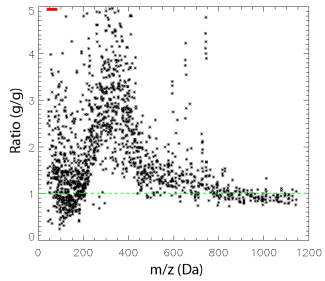

(g) 30 °C, 15 L min^{-1}, 21 min [1.640; 1.570]

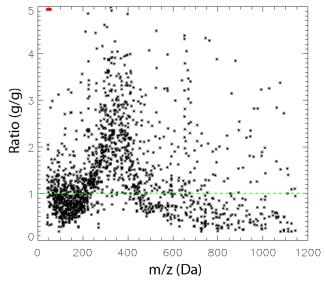

(h) 40 °C, 15 L min^{-1}, 20 min [1.155; 1.195]

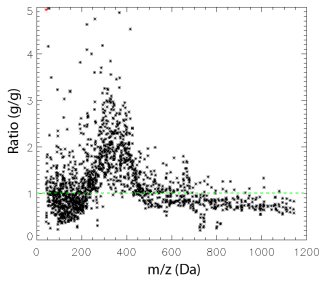

(i) 50 °C, 15 L min^{-1}, 18 min [1.085; 0.795]

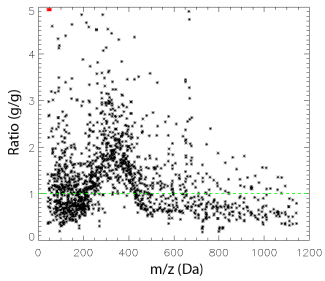

(j) 30 °C, 20 L min^{-1}, 17 min [1.180; 0.985]

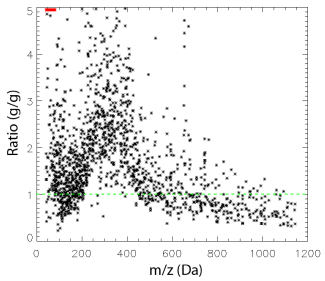

(k) 40 °C, 20 L min^{-1}, 11 min [1.600; 1.440]

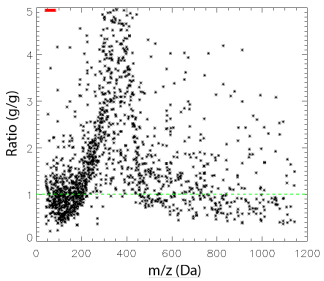

(l) 50 °C, 20 L min^{-1}, 15 min [1.400; 1.565]

Figure 14: Axis as in figure 12. The comparison PTR-ice:liquid and PTR-ice:dry are compared under different evaporation conditions. In the caption is the evaporation temperature, flow and duration given, respectively.

4.3 Tackling surface artifacts: First attempts

4.3.1 The setup

Both in section 4.1 and 4.2 a mean loss of mass loading was reported over the majority of ions when compared to the TD-PTR-MS measurements.
Therefore, measurements with a more inert surface area are preferred. A cone-like shape will be used for this, as can be seen in figure 15. It is made with PFA (perfluoroalkoxy film, 0.05 mm thickness, HP Products, The Netherlands) which is welded together with a heat sealer (381PS Audion Elektro, The Netherlands). The welding lines are indicated by thick black lines in the figure. The inclusion of a chamber by the two triangular placed welding-lines in the cone enhances evaporation when dry air flows through. The sample remains in the lowest part of the cone, as is indicated.
The cone is cleaned with a dry air flow containing 0.1 ppb ozone with a 2.0 L min^{-1} flow for 15 minutes long. After this, the sample is inserted in the l.h.s. of the cone. The l.h.s. is attached with iron wire to the dry air source after which a 20 L min^{-1} flow, under a controlled temperature of 30 °C, is used to evaporate the water. Afterwards, the r.h.s. is attached with iron wire to the PTR-ToF-MS while the entire cone is under temperature controlled conditions, which is shown schematically in figure 16. An aluminium chamber is installed with an opening towards a heater. The PTR-cone is indicated by the oval shape inside the aluminium chamber.
Since both the isolation layer and the inside of the aluminium chamber consists of (heated) ambient air, there is direct contact between the hot air provided by the heater and the cone and the heat is unevenly distributed throughout the inside of the aluminium chamber. The maximum working temperature is therefore restrained to a lower temperature than ultimately possible with PFA. A maximum operating temperature of 150 °C was found. Measurements will be taken from an initial temperature of 50 °C to a maximum of 150 °C with an increasing temperature rate of 13 °C min^{-1}. Measurement of the temperature has been done by a thermocouple which was held in the hot airflow. The filter with sample code 89 is used. The sample is mixed with 2.0 mL of milliQ-water. Measurements proceeded as described in appendix C. The cones are cleaned with a 2 L min^{-1} flow containing 0.1 ppb O_3 for 15 min. Afterwards, the sample is inserted to the cone. The moisture is evaporated with a 20 L min^{-1} dry air flow, which takes approx. 2 h. The N_2-flow is controlled at 50 mL min^{-1} after which the measurement takes place with the temperature increasing to 150 °C, as has been mentioned above.

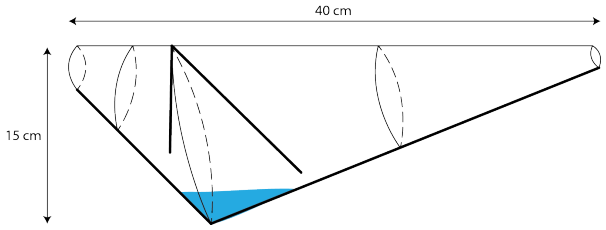

Figure 15: PFA cone with the four indicated welding lines (thick black line). In/outlets are at the most left and most right side. For illustrative purposes, A blue triangle imitating water is included in the figure.

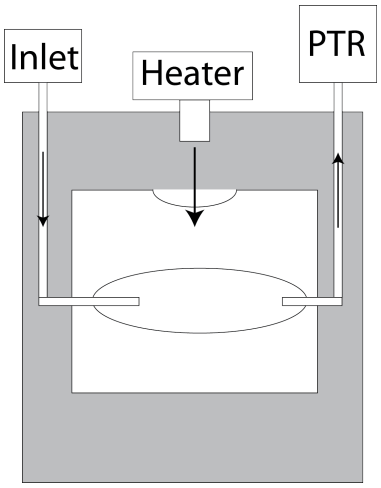

Figure 16: Schematic top-view of the setup for measurements with the PTR-cone.

4.3.2 Measurement

A total of 4376 ions were discriminated, of which around 2800 ions have little mass load when measured with TD-PTR-MS (less than 0.5 ng cm^{-2}). In figure 17 three replicate measurements of the PTR-cone:dry are shown. The measurement on the left and the measurement on the right show a good comparison as they have a median value around 1 (0.980 and 1.025) and the median 50% are scattered around this value (both 0.195), where the middle measurement is a clear outlier (median 1.830 and scatter 3.625). The cone

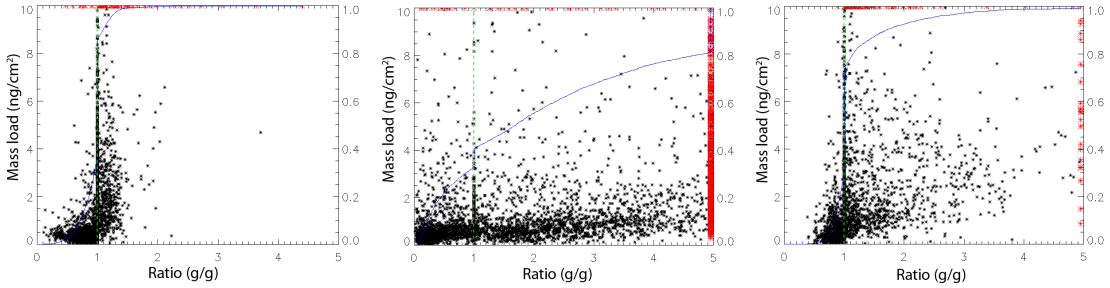

(a) PTR-cone:dry &PTR-cone:dry. Sample 89. [0.980;0.195]

(b) PTR-cone:dry &PTR-cone:dry. Sample 89. [1.830;3.625]

(c) PTR-cone:dry &PTR-cone:dry. Sample 89. [1.025;0.195]

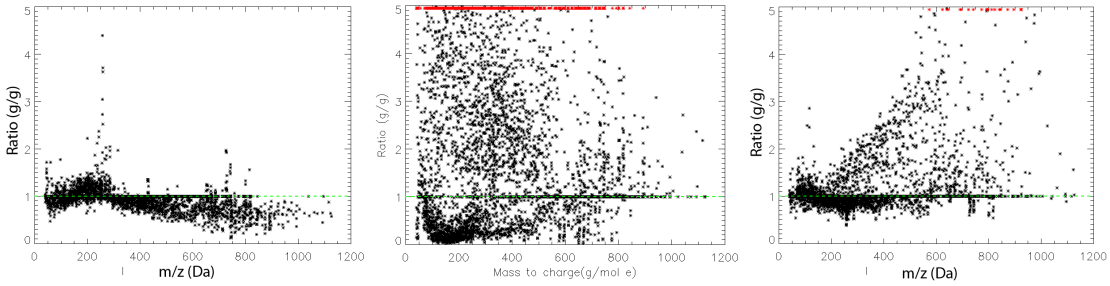

(d) PTR-cone:dry &PTR-cone:dry. Sample 89.

(e) PTR-cone:dry &PTR-cone:dry. Sample 89.

(f) PTR-cone:dry &PTR-cone:dry. Sample 89.

Figure 17: Axis as in figure 12 with the horizontal scale adjusted (ratio from 2.0 to 5.0). The intercomparison of three replicate measurements is shown. The three individual measurements are compared to the median value of the three measurements. The measurement with the PTR-cone:dry is compared.

used for this measurement was slightly molten during the measurement, being a likely explanation for this measurement to be an outlier. For further analysis the middle measurement is no longer regarded. The possibility of contamination in our measurements due to melting of the cones should, however, be kept in mind.

In figure 18 (left) the comparison between the PTR-cone and the TD-PTR-MS is shown. The comparison between PTR-cone:dry and TD-PTR-MS results in ratio's around the expected value of 1. Although the scatter in ratio's detected around the median value is increased (to 2.120) with respect to the PTR-ice method (which has a scatter of approximately 0.3), 1092 organics are within ±0.2 from the ratio of 1.0, which is approximately 25% of all organics measured. In figure 18c, compounds with a m/z-value of over 500 Da have an increased ratio. When we regard only the organics with a m/z-value lower than 500 Da, we get a median value of 0.985 with the median 50% of these organics measured within maximum difference in ratio of 0.750. When we compare the entire m/z-range with the replicate measurements individually, we obtain the characteristics of $[1.145; 1.615]$ and $[1.130; 2.44]$ (as in the caption of the figure, the first number is the median ratio and the second number is the maximum difference in ratio's for the median 50%). Both are in agreement to the measurement where we have used the mean of the two, $[1.140; 2.120]$. An extra form of contamination is introduced with the measurement in PTR-cone. This occurs above the 500 Da-range. No direct comparison between the TD-PTR-MS measurement and PTR-cone should therefore be made above this mass to charge range. Since consistency remains in the organics with a lower m/z-value, a comparison of the measurement of these organics between TD-PTR-MS and PTR-cone can be made. 646 different compounds are found to have a ratio of above 5.

When regarding the comparison of PTR-cone:liquid to PTR-cone:dry (right) a median ratio of 1.235 has been found. The spread, however, is larger with a difference of the minimum and maximum ratio of the median 50% of 4.590. The compounds with a m/z-value below 400 Da are not well detected in this measurement. The same occurred in section 4.1. The time necessary to evaporate the water, approximately 2 h, may therefore be too long. 1434 different compounds are found to have a ratio of over 5.

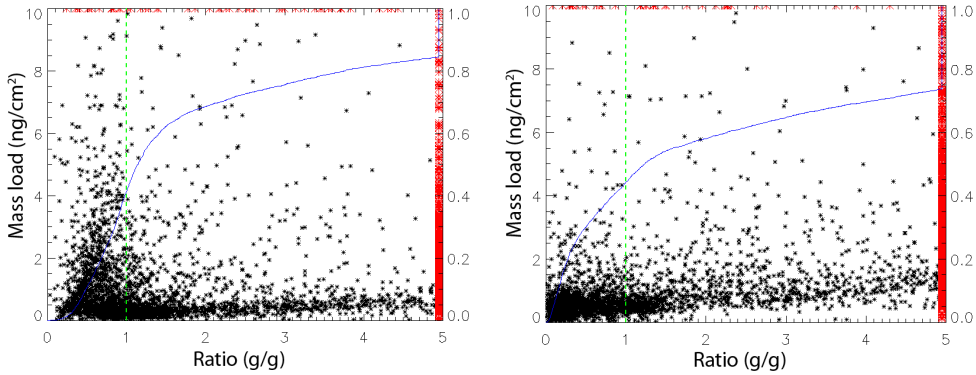

(a) PTR-cone:dry & TD-PTR-MS [1.140; 2.120]

(b) PTR-cone:liquid & PTR-cone:dry [1.235; 4.590]

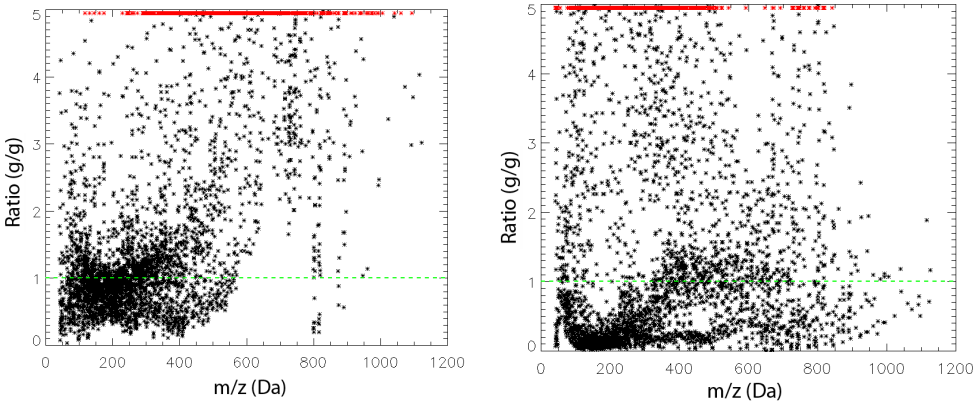

(c) PTR-cone:dry & TD-PTR-MS

(d) PTR-cone:liquid & PTR-cone:dry

Figure 18: The axis as in figure 12 with the horizontal scale adjusted (ratio from 2.0 to 5.0). The comparison between different measurement methods using the PTR-cone is shown.

4.3.3 Conclusion

The fraction of particles that recondensate on the surface are has been reduced by using a more inert surface. The loosely fixed thermocouple may indicate an incorrect temperature and therefore the test series is limited by poor temperature control. Approximately 25% of all organics measured are nonetheless found to be within ± 0.2 around a ratio of 1.0 when comparing PTR-cone:dry to the TD-PTR-MS. For 646 different compounds, a ratio of over 5 was found. Despite these high valued ratios a median value of 1.140 was found for the comparison between PTR-cone:dry and TD-PTR-MS with a median 50% maximum-minimum difference of 2.120, which is under high influence of the organics with a m/z-value of over 500 Da. Results show an increase in the measured mass load for the inert PTR-cone with respect to the PTR-ice. The spread in the ratio's for the different organics, however, are larger than for the PTR-ice.
The comparison between PTR-cone:liquid and PTR-cone:dry was possibly under influence of the evaporation of water. With a higher evaporation efficiency and thus reducing it's duration, the organic compounds measured may show higher similarity to the measurement of a dry sample.

5 Conclusion and outlook

The global radiative forcing is relatively uncertain due to the unknown past aerosols composition. To obtain a clear image on the effects of particulate matter in the atmosphere to the Earth's mean temperature higher understanding of the past composition is necessary. A large unknown part of the aerosol species are the organic species, which can be measured with the PTR-ToF-MS. In this study a method was sought that enables us to measure organic compounds from ice samples, both the insoluble as the water soluble part.
A PTR-ice device, which was developed for this goal, was tested for it's measurement accuracy by comparing it to offline TD-PTR-MS measurements. Ambient filter samples from the CESAR observatory were used to provide sample replicates with which both methods could be compared.
The measurements done with the PTR-ice resulted in an approximate 56% loss of total mass load measured when compared to the TD-PTR-MS. When water was introduced, the decline in measured mass load decreased even further. Especially compounds with a low m/z-value (of below 400 Da) were found to be measured with a marginal mass load compared to the TD-PTR-MS. 549 organics with less than $0.2\,\mathrm{g\,g^{-1}}$ below 400 Da and 14 organics below $0.2\,\mathrm{g\,g^{-1}}$ above it. Due to both a considerable loss by the evaporation of water and an overall low mass load a twofold of possibilities to improve the PTR-ice were identified:

- Removal of bulk water
- Effects of surface artefacts

The challenges were tackled successively in sections 4.2 and 4.3. It was shown that when evaporation occurred with a dry air flow instead of with a vacuum pump, the losses were reduced significantly. A dry air flow of $10\,\mathrm{L\,min^{-1}}$ with a temperature of 30 °C resulted in the most favourable measurements. From a median ratio of 0.192 by using a vacuum pump to a median ratio of 1.195 by using dry air evaporation with an increase in the difference between the maximum and minimum ratio of the median 50% of all organics of 0.426 to 0.935. An unexpected high mass load was found at a m/z-value of about 300 Da, due to the possible contaminating dry air flow.
The effects of surface artefacts were discovered by using a custom made PFA cone in which the sample was inserted to increase the inertness of the surface area. Although not a measurement of the full temperature spectrum could be achieved, an increase in the mass load of multiple organics were found. Where initially a median ratio for the PTR-ice:dry compared to the TD-PTR-MS of 0.444 was obtained, with the adjustments to a more inert surface, the median ratio for the PTR-cone:dry compared to the TD-PTR-MS was now found at 1.140. Although the spread of the median 50% has increased from 0.212 to 2.120. An indication that improvements could be achieved when maintaining a more inert surface to the overall losses of mass load. Organics with a m/z-value of above 500 Da were overestimated in the measurements (a median ratio of 4.610 was found for $\mathrm{m/z} > 500\,\mathrm{Da}$).
The PTR-cone:liquid measurement was possibly under influence of the duration of the evaporation process. The compounds measured showed either a large loss of mass load or a high increase of mass load. This results in a ratio compared to PTR-cone:dry measurement-spread of the median 50% to be 4.590. For further liquid sample measurements with the PTR-cone, adjustments to the shape of the cone to enhance evaporation should be made.
The PTR-ice setup, initially with a vacuum pump evaporation, showed two possibilities of improvement. The first was the removal of bulk water which was improved by the use of a dry air flow instead of a vacuum evaporation. This increased the median ratio of the mass load to a factor 5. It came at the cost of a doubling of the spread of the median 50%. The improvement for the overall loss in the PTR-ice, which was seen in the PTR-ice:dry measurement, was discovered by the use of a more inert surface, PFA cones. The median ratio of the mass load compared to the TD-PTR-MS measurements increased from 0.444 to 1.140. At the cost of increasing the spread of the median 50% by a factor ten. Measurements with a more inert surface show promising results, that could, combined with the dry air evaporation, significantly improve the measurements of the PTR-ice which enables the measurement of glacier samples.

References

van Beelen, A. J. and van Delden, A. J. (2012). Cleaner air brings better views, more sunshine and warmer summer days in the Netherlands. *Weather*, 67(1):21–25.

Boucher, O., Randall, D., Artaxo, P., Bretherton, C., Feingold, G., Forster, P., Kerminen, V.-M., Kondo, Y., Liao, H., Lohmann, U., Rasch, P., Satheesh, S., Sherwood, S., Stevens, B., and Zhang, X. (2013). 2013: Clouds and Aerosols. In Stocker, T., Qin, D., Plattner, G.-K., Tignor, M., Allen, S., Boschung, J., Nauels, A., Xia, Y., Bex, V., and Midgley, P., editors, *Climate Change 2013: The Physical Science Basis. Contribution of Working Group I to the Fifth Assessment Report of the Intergovernmental Panel on Climate Change*. Cambridge University Press, Cambridge, United Kingdom and New York, NY, USA.

Brunekreef, B. and Forsberg, B. (2005). Epidemiological evidence of effects of coarse airborne particles on health. *European Respiratory Journal*, 26(2):309–318.

Dentener, F., Kinne, S., Bond, T., Boucher, O., Cofala, J., Generoso, S., Ginoux, P., Gong, S., Hoelzemann, J. J., Ito, A., Marelli, L., Penner, J. E., Putaud, J.-P., Textor, C., Schulz, M., van der Werf, G. R., and Wilson, J. (2006). Emissions of primary aerosol and precursor gases in the years 2000 and 1750 prescribed data-sets for AeroCom. *Atmospheric Chemistry and Physics*, 6(12):4321–4344.

Dotan, I., Albritton, D., Lindinger, W., and Pahl, M. (1976). Mobilities of co2+, n2h+, h3o+, h3o+. h2o, and h3o+.(h2o) 2 ions in n2. *Journal of Chemical Physics*, 65:5028–5030.

Doyle, M. and Dorling, S. (2002). Visibility trends in the UK 1950 - 1997. *Atmospheric Environment*, 36(19):3161 – 3172.

Gelencsér, A. (2004). *Carbonaceous Aerosol*. Atmospheric and Oceanographic Sciences Library. Springer.

de Gouw, J. and Warneke, C. (2007). Measurements of volatile organic compounds in the Earth's atmosphere using Proton-Transfer-Reaction Mass Spectrometry. *Mass Spectrometry Reviews*, 26(2):223–257.

Grosjean, D. and Seinfeld, J. H. (1989). Parameterization of the formation potential of secondary organic aerosols. *Atmospheric Environment (1967)*, 23(8):1733 – 1747.

Holzinger, R., Kasper-Giebl, A., Staudinger, M., Schauer, G., and Röckmann, T. (2010a). Analysis of the chemical composition of organic aerosol at the Mt. Sonnblick observatory using a novel high mass resolution thermal-desorption proton-transfer-reaction mass-spectrometer (hr-TD-PTR-MS). *Atmospheric chemistry and physics*, 10(20):10111–10128.

Holzinger, R., Williams, J., Herrmann, F., Lelieveld, J., Donahue, N. M., and Röckmann, T. (2010b). Aerosol analysis using a Thermal-Desorption Proton-Transfer-Reaction Mass Spectrometer (TD-PTR-MS): a new approach to study processing of organic aerosols. *Atmospheric Chemistry and Physics*, 10(5):2257–2267.

IPCC (2013). 2013: Summary for Policymakers. In Stocker, T., Qin, D., Plattner, G.-K., Tignor, M., Allen, S., Boschung, J., Nauels, A., Xia, Y., Bex, V., and Midgley, P., editors, *Climate Change 2013: The Physical Science Basis. Contribution of Working Group I to the Fifth Assessment Report of the Intergovernmental Panel on Climate Change*. Cambridge University Press, Cambridge, United Kingdom and New York, NY, USA.

Izumi, K. and Fukuyama, T. (1990). Photochemical aerosol formation from aromatic hydrocarbons in the presence of {NOx}. *Atmospheric Environment. Part A. General Topics*, 24(6):1433 – 1441.

Legrand, M. and Mayewski, P. (1997). Glaciochemistry of polar ice cores: A review. *Reviews of Geophysics*, 35(3):219–243.

Pöschl, U. (2005). Atmospheric Aerosols: Composition, Transformation, Climate and Health Effects. *Angew. Chem. Int. Ed.*, 44:7520–7540.

Timkovsky, J., Dusek, U., Henzing, J., Kuipers, T., Röckmann, T., and Holzinger, R. (2014). Offline thermal-desorption proton-transfer-reaction mass spectrometry (TD-PTR-MS) technique as a method to study composition of organic aerosol. *Journal of Aerosol Science (submitted)*.

Viehland, L. and Mason, E. (1995). Transport properties of gaseous ions over a wide energy range, iv. *Atomic Data and Nuclear Data Tables*, 60(1):37–95.

A Procedure of measurement for PTR-ice

1. Initialise PTR-ice
   → Power supply on → First and second chamber temperature to 50 °C
2. PTR-MS shutdown/initialise
   Shutdown
   → Udrift: 0
   → IHC: Off
   → Close N2 valve
   → TPS controller: shutdown
   → H2O: 0
   Initialise
   → # writes: 90
   → Drift: 120 °C
   → Inlet: 180 °C
   → IhC: 6 mA
   → SV: 100
   → Tof time setting: 83340 waveforms (5 s)
   → Driftpressure: 2.8 (controlled)
   → Us: 140
   → Uso: 92
   → Udl: 35.0
   → FC inlet: 0
   Conditions
   → Pump attached to PTR-MS
   → TOF < 5 E-7 mbar
3. Start pump, check flow through air in/outlet. It should be 3 L min^{-1}.
4. Stop pump
5. Insert ice cube in first chamber
6. After 4 min the ice has melted, start pump.
7. The flow should be the same as the previously checked 3 L min^{-1}.
8. Evaporate the water. At a pressure of 31.0 mbar close the air in/outlet.
9. At a pressure of 2.1 mbar or after 20 min:
   → Start N_2-flow
   → Close valve to pump
   → At a pressure over 1 atm open air in/outlet
10. Close the valve towards the pump, shut down the pump after a couple of minutes.
11. Open the pressure release valve, check the outgoing flow
12. Start PTR-MS
    → Udrift: 600
    → IHC: On
    → H2O: 4.0 sccm
    → Reload TPS controller, initialise with latest settings
13. PTR-MS Begin measurement.
14. Start heating program after 2 min first chamber (EZ-button).
15. After 19 min start heating program second chamber (EZ-button)
16. After 33 min the measurement is done and the first and second chamber can be cooled down.
    → To 50 °C → Open top lid
    → Cool with liquid N_2
17. For a next measurement go back to step 2
18. After the last measurement of the day:
    → PTR-MS shutdown (check step 2)
    → Drift: 80 °C → Inlet: 50 °C
    → Udx: 0

B Procedure of measurement for PTR-ice with dry air

1. Initialise PTR-ice
   → Power supply on → First and second chamber temperature to 50 °C
2. PTR-MS shutdown/initialise
   Shutdown
   → Udrift: 0
   → IHC: Off
   → Close N2 valve
   → TPS controller: shutdown
   → H2O: 0
   Initialise
   → # writes: 90
   → Drift: 120 °C
   → Inlet: 180 °C
   → IhC: 6 mA
   → SV: 100
   → Tof time setting: 83340 waveforms (5 s)
   → Driftpressure: 2.8 (controlled)
   → Us: 140
   → Uso: 92
   → Udl: 35.0
   → FC inlet: 0
   Conditions
   → TOF < 5 E-7 mbar
3. Insert ice cube in first chamber
4. After 4 min the ice has melted, start dry air flow.
5. Control the temperature and flow rate of the dry air.
6. At a Relative Humidity of 6%:
   → Stop dry air flow
   → Start N_2-flow
7. Start PTR-MS:
   → Udrift: 600
   → IHC: On
   → H2O: 4.0 sccm
   → Reload TPS controller, initialise with latest settings
8. PTR-MS Begin measurement.
9. Start heating program after 2 min first chamber (EZ-button).
10. After 19 min start heating program second chamber (EZ-button)
11. After 33 min the measurement is done and the first and second chamber can be cooled down.
    → To 50 °C → Open top lid
    → Cool with liquid N_2
12. For a next measurement go back to step 2
13. After the last measurement of the day:
    → PTR-MS shutdown (check step 2)
    → Drift: 80 °C → Inlet: 50 °C
    → Udx: 0

C Procedure of measurement for PTR-cone

1. PTR-MS shutdown/initialise
   Shutdown
   → Udrift: 0
   → IHC: Off
   → Close N2 valve
   → TPS controller: shutdown
   → H2O: 0
   Initialise
   → # writes: 90
   → Drift: 120 °C
   → Inlet: 180 °C
   → IhC: 6 mA
   → SV: 100
   → Tof time setting: 83340 waveforms (5 s)
   → Driftpressure: 2.8 (controlled)
   → Us: 140
   → Uso: 92
   → Udl: 35.0
   → FC inlet: 0
   Conditions
   → TOF $<$ 5 E-7 mbar
2. Attach cone to inlet-tube.
3. Start dry air flow with ozone:
   → O_3 concentration: 0.1 ppb
   → Flow: 2 L min^{-1}
4. After 15 min stop dry air flow containing ozone.
5. Remove cone from inlet-tube
6. insert sample in the cone
7. Reattach cone to inlet-tube
8. Start a dry air flow of 20 L min^{-1}
9. Evaporate the water (approx. 2 h)
10. Stop dry air flow
11. Attach the cone to PTR-tube
12. Start N_2-flow (controlled at 50 mL min^{-1})
13. Start PTR-MS:
    → Udrift: 600
    → IHC: On
    → H2O: 4.0 sccm
    → Reload TPS controller, initialise with latest settings
14. PTR-MS Begin measurement.
15. Start heating program after 2 min PTR-cone (EZ-button).
16. For a next measurement go back to step 2
17. After the last measurement of the day:
    → PTR-MS shutdown (check step 2)
    → Drift: 80 °C
    Udx: 0
    → Inlet: 50 °C